

# IMPROVEMENTS IN FAKTOR2, A CODE TO SIMULATE COLLECTIVE EFFECTS OF ELECTRONS AND IONS

W. Bruns\*, D. Schulte, F. Zimmermann, CERN, Geneva, Switzerland

## Abstract

The electrostatic Particle in Cell code 'Faktor2' is extended to 3D, and is partly parallelised. Results for electron cloud buildup in wigglers and in end regions of damping ring dipoles for next generation linear colliders are presented.

## PURPOSE AND MODEL

Electron clouds develop in the beam pipes of accelerators eg. via photoelectrons and via secondary emission of electrons when slow electrons are accelerated by a passing beam. For an overview of these effects, see [1]. The newly developed programme simulates these effects. The basic method is electrostatic Particle in Cell.

The large number of freely moving charges (electrons) are replaced by a smaller number of macroparticles. Each macroparticle represents a large number of charges with the same ratio of charge/mass and nearby positions in phase space, ie nearly the same position and velocity. The equations of motion for these macroparticles are integrated according to NEWTON's law with the force given by the sum of the self field of the particles, the TEM-field of a relativistic beam, a magnetostatic field and an electrostatic field of clearing electrodes. At each timestep, the self field and the electrostatic field of electrodes is computed on a rectangular mesh. Each gridcell can be recursively refined, where each refinement step decreases the grid spacing by a factor of two, see fig. 1. The TEM-field of an arbitrarily shaped relativistic bunch is also computed on that mesh.

## PARALLELISATION

The computational load consists of three parts. A: For each grid point, the charge of the macroparticles near the point is summed up to give the right hand side of POISSON's equation. B: POISSON's equation is solved on the grid, giving the electrostatic potential and from that the self force and the force due to electrodes. C: For each macroparticle the equation of motion is integrated over the timestep. The computational loads of steps A and C are proportional to the number of macroparticles. These steps are parallelised by distributing the macroparticles evenly over the available processors. The step B, solving POISSON's equation is not yet parallelised, but is performed via a multigrid algorithm. It's computational load is proportional to the number of gridcells. A speedup of three when

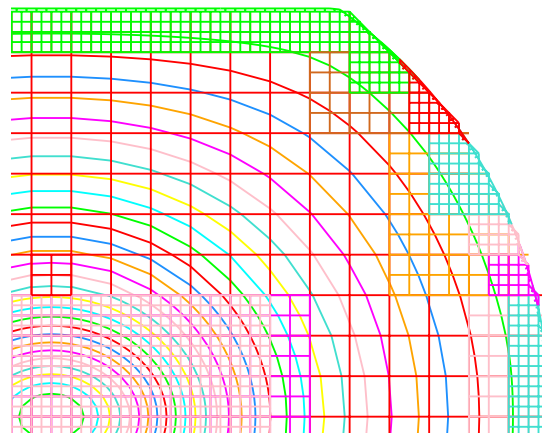


Figure 1: Subdivision of the grid near the pipe boundary and at the location of the beam. Two levels of refinement are applied. The different colours of the refined cells indicate clusters of cells which are treated as rectangular grids. The curved lines are lines of constant potential of an elliptical beam at the center.

four CPUs are used is achieved with this partly parallelisation.

## MODELLING OF SCRUBBING

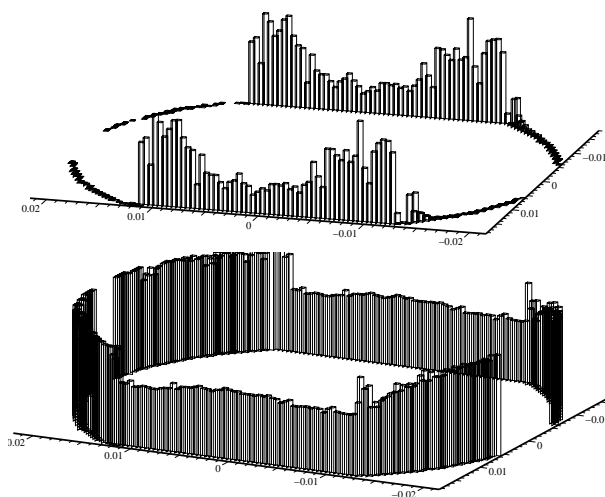


Figure 2: Above: Integrated dose of electron hitting the wall. Below: New SEY estimate computed from the dose.

The secondary emission yield (SEY) of a material depends on the history [2]. This is called scrubbing. Faktor2 can report the amount of charge that has hit a particular

\*This work is supported by the Commission of the European Communities under the Framework Programme "Structuring the European Research Area", contract number RIDS-011899

region of the beam pipe. That data is used to estimate the SEY of that region. In a subsequent run, the SEY as a function of the position on the beam pipe is read from a datafile and is used for the next simulation. Fig. 2 shows the dose and the SEY estimate for a LHC-like beam pipe.

## RESULTS

### Electron Cloud in a Wiggler

We compute the buildup of electrons in a wiggler section with a geometric periodicity of 5 cm. The beam pipe cross section is 32 mm times 18 mm. The maximum  $B_y$  field is 2.4 Tesla. A photoelectron rate of  $4 \times 10^7$  photoelectrons per metre per bunch is assumed. The creation of secondary electrons is modeled with a secondary emission yield of 1.5 at 230 eV impact energy. The bunch train consists of 311 positive bunches with a population of  $4 \times 10^9$  elementary charges. The bunch spacing is 0.2 metres, the length of each bunch is  $\sigma = 1.5 \times 10^{-3}$  metres. The transverse extent of the bunches is much smaller than the grid spacing, therefore the bunches are modeled as line charges. Fig. 3 shows the computed electron density near the axis. For comparison, fig. 3 also shows the electron density in the same geometry, when a spatially constant magnetic field is assumed. Fig. 4 shows the power deposited by the electrons hitting the wall. Fig. 5 shows the charge density near the axis as a function of  $z$ , while fig. 6 shows the charge density near the axis as a function of  $s$ , ie. as a function of the offset from the moving beam. Fig. 7 shows the wakepotential due to the electron cloud.

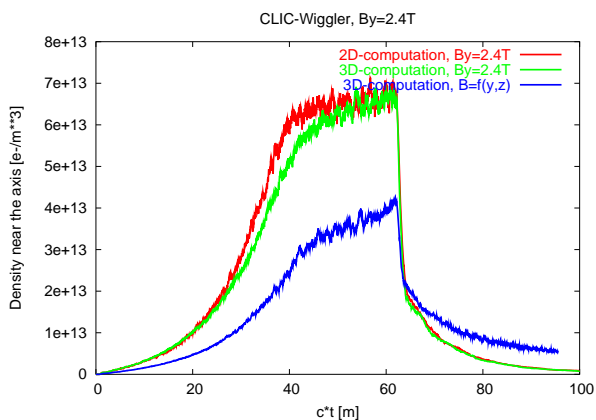


Figure 3: Time dependence of the electron density near the axis in a wiggler section with a period length of 5 cm. The transverse dimensions of the beam pipe are 32 mm times 18 mm. The amplitude of the wiggler field is 2.4 Tesla. Red curve: Result of a 2D computation, ie no  $E_z$ -fields are possible. Green: Result of a 3D-computation, but the wiggler field is assumed to be  $B_y=2.4$  Tesla everywhere. Blue: Result of a 3D-computation, where the Wigglerfield is a realistic 3D field with amplitude 2.4 Tesla.

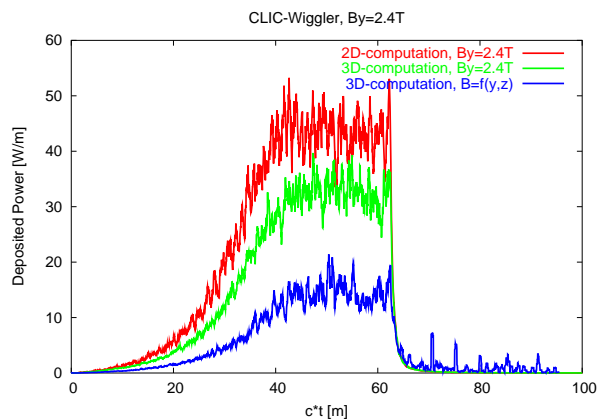


Figure 4: Time dependence of the Power deposited by the electrons hitting the wall. Red curve: Result of a 2D computation, ie no  $E_z$ -fields are possible. Green: Result of a 3D-computation, but the Wigglerfield is assumed to be  $B_y=2.4$  Tesla everywhere. Blue: Result of a 3D-computation, where the Wigglerfield is a realistic 3D field with amplitude 2.4 Tesla.

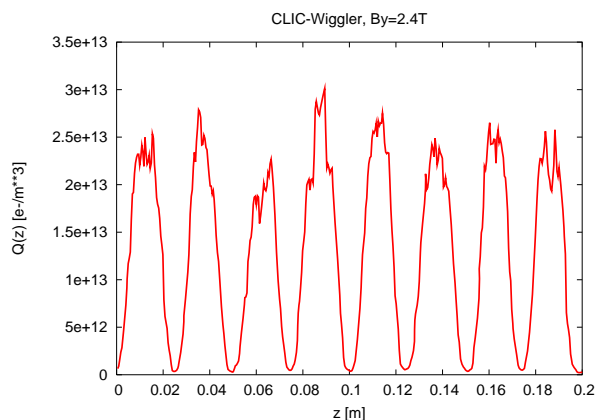


Figure 5: Time average of the electron density near the axis in the wiggler. The minima of the density occur at the zeros of the  $B_y$ -component. Four wiggler periods were modeled to also be able to model the periodic occurrence of the exciting charge, which has a periodicity of  $c*T = 0.2$  metres.

### End Region of Dipoles

The electron cloud buildup in the end region of a dipole is computed. The magnetostatic field is computed by applying BIOT-SAVART for a model of the currents. A photoelectron flux of  $4 \times 10^6$  electrons per bunch per metre is assumed. The creation of secondary electrons is modeled with a secondary emission yield of 1.5 at 230 eV impact energy. The bunch train consists of 311 positive bunches with a population of  $4 \times 10^9$  elementary charges. The bunch spacing is 0.2 metres, the length of each bunch is  $\sigma = 1.5 \times 10^{-3}$  metres. The transverse extent of the bunches is much smaller than the grid spacing, therefore the bunches are modeled as line charges.

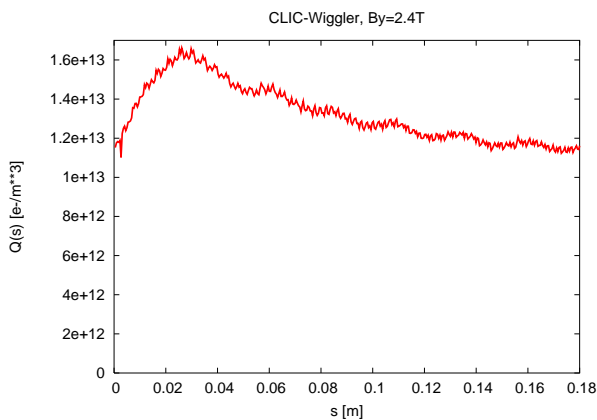


Figure 6: Time average of the electron density near the axis in the wiggler. Note that the abscissa is the distance from the beam. The charges near the beam are accelerated towards the beam, giving a density maximum at  $s=c*t=0.027$  m after the beam has passed.

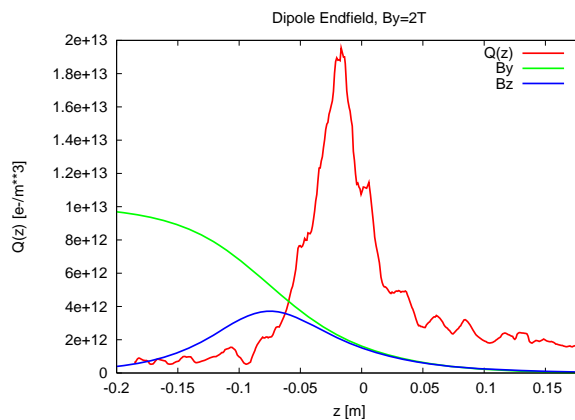


Figure 8: Time average of the electron density near the axis in the end region of a dipole. Red: Electron density. Green and blue: shape of the  $B_y$  and  $B_z$  component. The maximum of the charge density just after the endfield occurs because the electrons are directed via the  $B_z$  component towards this region, and concentrate near the axis. The higher density in the region where no magnetic field is occurs because all charges are accelerated towards the beam on the axis, and all trajectories come very near to the axis, as no magnetic field could bend the trajectories otherwise.

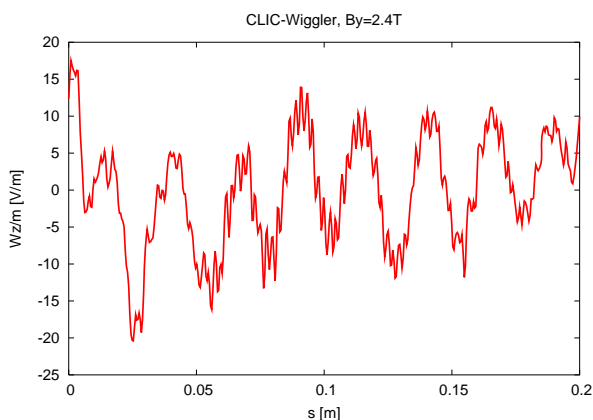


Figure 7: Wakepotential due to the electron cloud in the wiggler. The exciting bunches have a periodicity of 0.2 m, therefore the shown data repeats after 0.2 metres. The seen period length corresponds to the period of the magnetic field.

Fig. 8 shows the electron density near the axis as a function of  $z$ . The maximum density occurs just at the end region. In the field free region, a higher density occurs than in the dipole itself. Fig. 9 shows trajectories of macroparticles in a region of zero magnetic field. These trajectories explain the higher density: essentially all charges travel over the region near the axis.

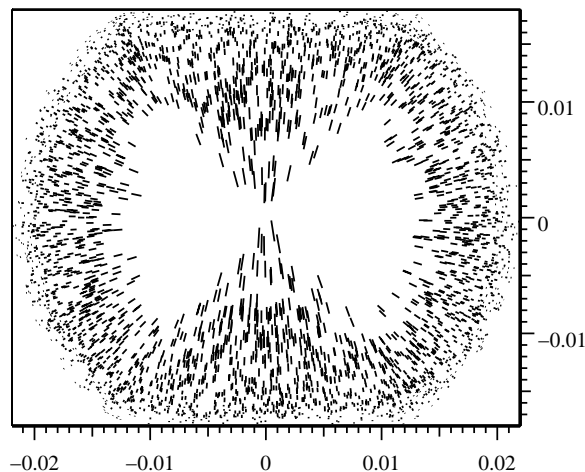


Figure 9: Trajectories of photoelectrons in a region of zero magnetic field. The electrons start near the beam pipes wall and are accelerated towards the positively charged beam. The shown trajectories are from photoelectrons created and accelerated by 8 bunches. The faster electrons were created by the first bunches and have been accelerated by all subsequent bunches. The slow electrons near the wall have just been created.

**SUMMARY AND AVAILABILITY**

A new electrostatic Electron cloud buildup code is applied to 3D configurations. The results are compared to 2D results. The code is written in Fortran-95 and has been successfully compiled and tested with several compilers on several architectures. The code is available from the authors.

**REFERENCES**

[1] Proc. ECLLOUD'04, Napa, CERN-2005-001 (2005)  
 [2] V. Baglin et al., "Measurements at EPA of Vacuum and Electron-Cloud Related Effects", Proceedings LHC Workshop - Chamonix XI, Jan. 2001, CERN-SL-2001-003 DI